Designing Transmembrane α-Helices That Insert Spontaneously†

William C. Wimley‡ and Stephen H. White*

Department of Physiology and Biophysics and the Program in Macromolecular Structure, University of California at Irvine, Irvine, California 92697-4560

Received November 30, 1999; Revised Manuscript Received February 1, 2000

ABSTRACT: Direct measurement of the free energies of transfer of hydrophobic membrane-spanning α-helices from water to membranes is important for the determination of an accurate experiment-based hydrophobicity scale for membrane proteins. An important objective of such a scale is to account for the presently unknown thermodynamic cost of partitioning hydrogen-bonded peptide bonds into the membrane hydrocarbon core. We describe here the physical properties of a transmembrane (TM) peptide, TMX-1, designed to test the feasibility of engineering peptides that spontaneously insert across bilayers but that have the important property of measurable monomeric water solubility. TMX-1, Ac-WNALAAVAAAL-AAVAAALAAVAAGKSKSKS-NH_2, is a 31-residue sequence with a 21-residue nonpolar core, N- and C-caps to favor helix formation, and a highly polar C-terminus to improve solubility and to control directionality of insertion into lipid vesicles. TMX-1 appeared to be soluble in water up to a concentration of at least 1 mg/mL (0.3 mM). However, fluorescence spectroscopy, fluorescence quenching, and circular dichroism (CD) spectroscopy indicated that the high solubility was due to the formation of molecular aggregates that persisted at peptide concentrations down to at least 0.1 μM peptide. Nevertheless, aqueous TMX-1 partitioned strongly into membrane vesicles with apparent mole-fraction free-energy values of −7.1 kcal mol^{-1} for phosphatidylcholine (POPC) vesicles and −8.2 kcal mol^{-1} for phosphatidylglycerol (POPG) vesicles. CD spectroscopy of TMX-1 in oriented multilayers formed from either lipid disclosed a very strong preference for a transmembrane α-helical conformation. When TMX-1 was added to preformed vesicles, it was fully helical. A novel fluorescence resonance energy transfer (FRET) method demonstrated that at least 50% of the TMX-1 insered spontaneously across the vesicle membranes. Binding and insertion were found to be fully reversible for POPC vesicles but not POPG vesicles. TMX-1 was thus found to have many of the properties required for thermodynamic measurements of TM peptide insertion. Importantly, the results obtained delineate the experimental problems that must be considered in the design of peptides that can partition spontaneously and reversibly as monomers into and across membranes. Our success with TMX-1 suggests that these problems are not insurmountable.

Of the many thousands of protein sequences in the rapidly growing list of genomic databases, roughly a third are thought to be membrane proteins (*2*−*4*). Many of these, however, have not been unequivocally identified as such and thus their structure and function remain unknown. Compared to soluble proteins, the prediction of the structure of membrane proteins (MPs), especially those comprising TM[1] α-helices, has long been assumed to be a simpler problem because of the topological and physicochemical constraints imposed by the membrane lipid bilayer (*5*−*9*). Indeed, hydropathy (HΦ) plots that take advantage of these constraints are arguably the single most successful protein structure prediction algorithm. Nevertheless, while HΦ plots easily recognize as significant peaks the most nonpolar regions of a protein sequence, the unequivocal assignment of peaks as true TM α-helical segments remains problematic. One reason for this is the nature of the commonly used hydrophobicity scales. There are two fundamental difficulties. First, the scales are connected only loosely to experimental measurements. Various authors have adapted a limited amount of experimental data to accommodate their perceptions and observations about the relative energetic importance of side-chain physical properties. Because MPs are apparently equilibrium structures (reviewed in refs *1* and *10*), proper scales should be based upon direct, experimental determinations of membrane partitioning under equilibrium conditions. Second, they are side-chain-only scales and thus thermodynamically incomplete. A growing body of evidence indicates that the free energy ΔG_{Hbond} associated with dehydration of the H-bonded peptide bond has a major effect on the energetics of folding both soluble (*11*−*14*) and membrane proteins (*15*−*17*). The extreme importance of accounting for

† This research was supported in part by a grant from the National Institute of General Medical Science (GM-46823).

* To whom correspondence should be addressed: Phone 949-824-7122; FAX 949-824-8540; E-mail SHWhite@uci.edu.

‡ Present address: Department of Biochemistry SL-43, Tulane University Medical School, New Orleans, LA 70112.

[1] Abbreviations: CD, circular dichroism; OCD, oriented circular dichroism; TM, transmembrane; MP, membrane protein; HΦ, hydropathy or hydrophobicity. LUV, large unilamellar vesicles (diameter ∼0.1 μm); POPC, 1-palmitoyl-2-oleoyl-*sn*-glycero-3-phosphocholine; POPG, 1-palmitoyl-2-oleoyl-*sn*-glycero-3-phosphoglycerol; LysoMC, *N*-(7-hydroxyl-4-methylcoumarin-3-acetyl)-1-palmitoyl-2-hydroxy-*sn*-glycero-3-phosphoethanolamine; TMX-1, Ac-WNALAAVAAALAA-VAAALAAVAASKSKSKSK-NH_2; NBD-PE, *N*-(7-nitrobenz-2-oxa-1,3-diazol-4-yl)-1-palmitoyl-2-oleoyl-*sn*-glycero-3-phosphoethanolamine; 7-doxyl-PC, 1-palmitoyl-2-(7-doxylstearoyl)-*sn*-glycero-3-phosphocholine; RET, resonance energy transfer.

10.1021/bi992746j CCC: $19.00 © 2000 American Chemical Society
Published on Web 03/22/2000

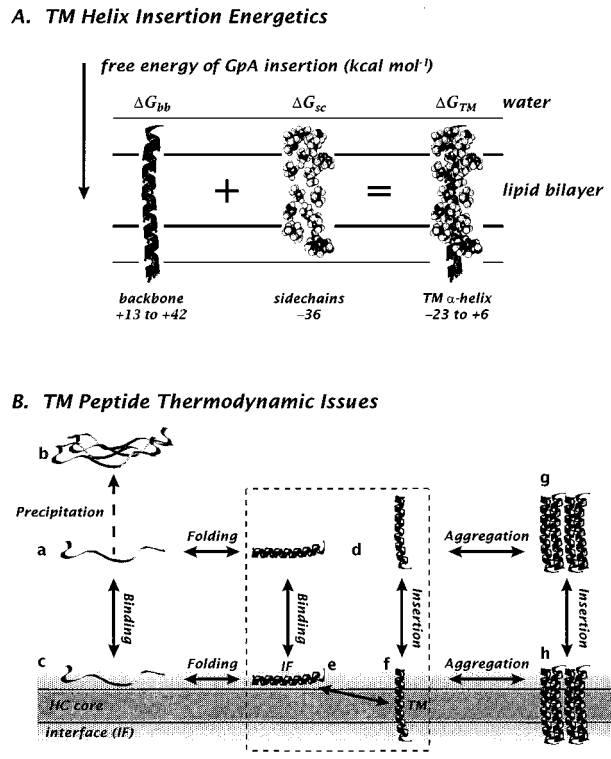

FIGURE 1: Determinants of the free energy of insertion of TM helices and thermodynamic issues associated with the experimental determination of the free energy (reviewed in ref *1*). (A) The free energy change ΔG_{TM} ($\equiv \Delta G_{whf}$, see ref *1* and footnote 2) associated with inserting a glycophorin A (GpA) α-helix into and across a lipid bilayer is determined by the cost of dehydrating the H-bonded peptide bonds of the backbone (bb) as well as the side chains (sc). Except for two recent ones (*1*), hydrophobicity scales invariably ignore the important energetic cost of dehydrating the bb. For GpA, whose structure is represented in the figure [PDB code 1AFO (*67*)], ΔG_{sc} is estimated to be a very favorable -36 kcal mol^{-1} from the sc octanol scale of Wimley et al. (*13*). Estimates for the unfavorable cost of partitioning a single H-bonded peptide bond (ΔG_{Hbond}) range from 0.6 to 2.0 kcal mol^{-1} (reviewed in ref *1*), leading to values of ΔG_{bb} of 13−42 kcal mol^{-1}. The computed cost for ΔG_{whf} thus ranges from -23 to $+6$ kcal mol^{-1}. Accurate experimentally determined values for ΔG_{Hbond} and ΔG_{bb} are clearly essential for the accurate prediction of ΔG_{whf} and for placing hydropathy plots on an absolute energetic scale. (B) Summary of the problems associated with the direct experimental determination of ΔG_{whf} that arise primarily from the tendency of hydrophobic peptides to aggregate in the aqueous phase. A more complete thermodynamic description of peptide binding and insertion is presented in a recent review (*1*). An abbreviated discussion can be found at http://blanco.biomol.uci.edu.

ΔG_{Hbond} in hydrophobicity scales is evident from our experimentally determined whole-residue hydrophobicity scales for membrane interfaces (*16*) and *n*-octanol (*13*).

As summarized in Figure 1A, the unfavorable free energy ΔG_{bb} of dehydrating the peptide backbone is quite comparable to the favorable free energy ΔG_{sc} associated with side-chain partitioning. Furthermore, because of the uncertainty in the actual value of ΔG_{bb}, the absolute value for the partitioning free energy ΔG_{TM} for the TM helix is uncertain by ~20 kcal mol^{-1}! This means that ΔG_{TM} cannot be placed on an absolute thermodynamic scale in HΦ plots unless the peptide bonds are accurately accounted for in hydrophobicity scales. When an absolute scale is used, the $\Delta G = 0$ level is expected to mark the "acceptance" level for designating an HΦ peak as a TM helix. The value of ΔG_{Hbond} consequently has a major influence on the prediction of TM helices from

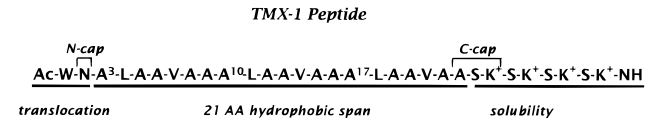

FIGURE 2: Sequence and design features of TMX-1. TMX-1 has a putative membrane-spanning 21 residue hydrophobic span surrounded by strong helical capping residues (*23*, *24*). The bulkier Leu and Val residues are situated at (i, $i + 3$) and (i, $i + 4$) in order to make the hydrophobic cross-section of the span asymmetric. The amidated C-terminus carries four positive charges to increase peptide solubility and to make the C-terminus membrane-impermeant. The uncharged acetylated N-terminus carries a Trp residue, expected to enhance membrane insertion, that was utilized as a spectroscopic probe for studies of peptide aggregation, membrane binding, and TM insertion.

HΦ plots (see refs *1* and *8* for detailed discussions). Determination of its exact value from measured TM-helix insertion free energies is thus an important experimental goal. Several notable attempts (*18*−*21*) have been made to determine these free energies, but all have been plagued by problems related to the complexities of the thermodynamic issues summarized in Figure 1B (reviewed in refs *1* and *22*). To clarify the experimental problems and to develop strategies for overcoming them, we have carried out a systematic study of a peptide (TMX-1) designed to insert spontaneously into lipid bilayers from the aqueous phase as a TM α-helix. The results are presented here.

Design Features of TMX-1. The primary ingredient required for experimental determination of a TM-helix whole-residue hydrophobicity scale is a family of host−guest peptides for which it is possible to measure the equilibria among peptides in water, membrane interface, and across the membrane (Figure 1B). The members of the family must be soluble in water as monomers, insert spontaneously as transmembrane helices, and bind strongly and reversibly to membranes. The simplest (easiest to interpret) case would be a peptide that partitions into the membrane only as a TM helix but is fully helical in water (d ⇔ f, dashed box in Figure 1B). If precipitation (a ⇔ b) and aggregation (d ⇔ g, f ⇔ h) can be avoided, the more likely case is a peptide that is partially helical in the aqueous phase and partitions both into the membrane interface (IF) and across the bilayer (a ⇔ d ⇔ e ⇔ f and/or a ⇔ c ⇔ e ⇔ f). To arrive at the desired d ⇔ f equilibrium in such a case, a careful accounting of the populations of each state is required. The peptide we describe here, TMX-1, is an exploratory peptide designed as an attempt to achieve the simplest case, but which turned out to be an example of g ⇔ f, g ⇔ h, or a combination of the two.

The sequence and design features for TMX-1 are summarized in Figure 2. We chose a minimally hydrophobic core with 21 consecutive hydrophobes (15 alanines, 3 leucines, and 3 valines) with the idea of increasing water solubility as much as possible without sacrificing the possibility of a transmembrane topology. The bulky Val and Leu residues were put at alternating (i, $i + 3$) and (i, $i + 4$) positions in order to concentrate them along one face of the presumed helix. This asymmetric arrangement was expected to promote both helicity on the membrane surface and the transition from a surface to a transmembrane state by favoring deeper insertion. To increase further the propensity for helices, we acetylated the N-terminus, amidated the C-terminus, and

flanked the hydrophobic core with strong helix-capping residues: Asn at the N-terminal side and a Ser-Lys-Ser sequence on the C-terminal side (*23*, *24*). The AGADIR algorithm (*25*−*28*) (http://www.heidelberg-embl.de/Services) predicts an average helicity of about 65% for TMX-1 in water under our conditions, with the central residues (Val^{7}−Ala^{19}) of the hydrophobic core exceeding 90% helicity. The four C-terminal serines and lysines (*29*) were included in order to increase the solubility of the peptide in water and to prevent the translocation of the C-terminus across membranes. AGADIR suggests an average helicity of ∼15% for this region. Finally, the N-terminal tryptophan was included as a presumed aid to insertion (*30*, *31*) but more importantly to allow for spectroscopic detection of insertion by fluorescence quenching methods.

As we describe below, TMX-1 had most of the properties envisioned such as nonprecipitation, strong helicity, reversible membrane binding, and a TM configuration. Its only shortcoming was that it formed molecular aggregates in the aqueous phase, which gave it a high apparent aqueous solubility. An important result of this work is that detection of such aggregates is an important step in validating measurements of TM helix insertion energetics. Our overall success with TMX-1 suggests that the experimental problems associated with thermodynamic measurements of TM peptide insertion are not insurmountable.

MATERIALS AND METHODS

Materials. POPC and POPG were purchased from Avanti Polar Lipids (Alabaster, AL). LysoMC was synthesized and purified as described in detail elsewhere (*32*). Large unilamellar vesicles of POPC and POPG (diameter = 1000 Å) were made by extrusion (*33*, *34*). The aqueous phase (pH 7) generally contained 10 mM HEPES, 50 mM KCl, 1 mM EDTA, and 3 mM NaN. For experiments involving CD spectroscopy, a 50 mM $KHPO_4$ (50 mM) buffer (pH 7) was used.

Synthesis of TMX-1. TMX-1 was synthesized on PEG-PS PAL by use of FMOC chemistry with a Milligen 9050 automated peptide synthesizer. The activity of the resin was reduced to ∼0.02 mmol/g in order to facilitate synthesis by reducing the potential for hydrophobic peptide interactions on the resin. Coupling was monitored with quinoline yellow and deprotection was monitored by UV absorbance. Deprotection was done with 30% piperidine in dimethylformamide (DMF) and was only about 2-fold slower at the end of the synthesis than at the beginning. Double coupling was used on all nonalanine residues after the first leucine. We cleaved the peptide under an argon atmosphere using 90% TFA, 5% thioanisole, 2.5% anisole, and 2.5% ethanedithiol. Cleavage was performed at 5 °C for the first 15 min and then at room temperature for an additional 3.5 h. The cleavage solution was filtered, dried under a stream of nitrogen, and extracted as a white precipitate into a water−dichloromethane mixture. The water phase and precipitate were lyophilized together and the product was relyophilized three times from glacial acetic acid, giving a slightly yellow, odorless powder.

Purification of TMX-1. Mass spectrum analysis of the crude product of the synthesis showed a single peak at the expected weight of 2821.6 Da with very few high molecular weight impurities. Crude peptide was first purified on a C18 reverse-phase HPLC column with 30% aqueous methanol + 0.1% TFA as the initial mobile phase[2] and 1:1 methanol/2-propanol + 0.1% TFA as the eluting phase. Of four large peaks, two were found to consist mostly of peptide with identical molecular masses (2821.6 Da). The peptides in the two fractions had identical retention times upon subsequent reverse-phase HPLC analysis, suggesting that the original two peaks were two different types of aggregates of the same peptide. Final purification was achieved by ion-exchange HPLC on a 0.45 × 5 cm poly-CAT-A weak anion-exchange resin following two cycles of reverse-phase HPLC. The highly cationic peptide was loaded onto the ion-exchange resin in 3:3:4 methanol/2-propanol/5 mM ammonium acetate (pH 6.7) and eluted with the same buffer containing 5% acetic acid. The final peptide was more than 95% pure and was stored in methanol at −20 °C.

Fluorescence. Fluorescence was measured on a SLM-Aminco 8100 steady-state fluorescence spectrometer. All measurements were made in 4 × 10 mm cuvettes at an ambient temperature of 22 °C. In all cases, polarizers were used in a magic angle configuration (excitation polarization set to 54.7° relative to vertical, emission polarization set to vertical) in order to correct for polarization effects in measurements of intensity, reduce direct contributions of light scattering, and eliminate polarization effects in monochromator transmittance. Tryptophan fluorescence was excited at 260 nm with slits set to 4 nm. For samples containing vesicles, the background intensity was scaled appropriately (*35*) and subtracted from the peptide-containing sample.

Potassium iodide quenching measurements were performed by titrating a 4 M solution of KI, stabilized with 2 mM sodium dithionite, into a peptide solution and measuring the intensity of fluorescence at 339 nm stimulated by excitation at 290 nm. Stern−Volmer quenching constants K_{S-V} were determined by linear regression with the equation $F_0/F = 1 + K_{S-V}[I]$, where F is the fluorescence intensity in the presence of iodide, F_0 is the fluorescence in the absence of iodide, and [I] is the molar concentration of iodide.

Determination of Peptide Concentration. TMX-1 concentration was routinely determined by quantitative ion-exchange HPLC (*36*) on a 0.45 × 5 cm HPLC column packed with Polycat-A weak ion-exchange resin (PolyLC Inc., Hamilton, ON). TMX-1 was loaded onto the column in 30% methanol/30% 2-propanol/40% 5 mM ammonium acetate at a flow rate of 3 mL/min and was eluted with the same buffer that also contained 5% acetic acid. Detection was at 280 nm. The amount of peptide in the injection was determined by comparing the peak area to that from standard solutions of TMX-1 or another cationic peptide, HNP-2 (*37*). Concentrations of the standards were determined by UV absorbance, amino acid analysis, or both.

Circular Dichroism Spectroscopy. Solution CD measurements were performed on a Jasco J-720 CD spectrometer with a 1 mm quartz cuvette and phosphate buffer. Peptide concentrations were between 2 and 20 μM in phosphate buffer. Lipid-containing samples had a concentration of 1.1 mM lipid in the form of POPC or POPG LUV. Scattering artifacts from the vesicles were minimal at wavelengths

[2] Solutions of methanol and trifluoroacetic acid (TFA) must never be used with peptides containing free carboxyl groups because the carboxyl moieties are rapidly O-methylated. TMX-1, however, contains no free carboxyl groups.

above 197 nm (*38*). At least 20 scans were collected and averaged for each sample with a scanning rate of 20 nm/min, 1 nm slits, and a response time of 2 s. Calibration was routinely confirmed by use of a 1-camphor-3-sulfonic acid (CSA) standard solution of known molarity.

Oriented CD spectra were measured by use of oriented multibilayers deposited on a quartz plate following the procedures of Huang and colleagues (*39*−*41*). TMX-1 and lipid at peptide-to-lipid ratios of 1:10 to 1:50 were codissolved in methanol at concentrations of approximately 10 mg/mL (12 mM) lipid and 1−3 mg/mL (0.3−1 mM) peptide. Between 2 and 10 μL of the this stock solution was layered carefully onto a 1-cm diameter circular area in the center of a 2.5 cm quartz plate. Following solvent removal under a stream of nitrogen and hydration with warm air at ~100% relative humidity, the plate was mounted (sample-side inward) on the end of a tube sealed at the opposite end with a second quartz plate. Samples were hydrated through the vapor phase by placing a drop of water or saturated salt solution in the sample holder before sealing. When mounted in the CD spectrometer, the optical axis was normal to the two parallel quartz plates. Spectra were recorded at each of 8 rotations of 45° around the optical axis and the resulting spectra were averaged. Background signal was determined with the same amount of lipid, without TMX-1.

Determination of Peptide Topology in Vesicles. The topology of the peptide's tryptophan residue in membranes was determined with a novel resonance energy transfer method, described in detail elsewhere (*32*), that uses the lysolipid-linked quencher lysoMC. Briefly, the determination requires three measurements of tryptophan fluorescence: (1) in pure lipid vesicles, (2) in vesicles that have 1 mol % lysoMC distributed symmetrically in both lipid leaflets, and (3) in vesicles with 1 mol % lysoMC in the outer leaflet only (achieved by adding lysoMC as a micellar solution to unlabeled vesicles). Measurements 1 and 2 establish the intensities of unquenched fluorescence and maximally quenched fluorescence. When compared with these fluorescence intensities, the degree of quenching observed in measurement 3 yields the topology of the Trp residue: If the degree of quenching is the same in asymmetric and symmetric lysoMC-containing vesicles, then the Trp must be on the outer monolayer of the vesicles, whereas if the quenching in the asymmetric vesicles is very low, then the Trp must be predominantly on the inside monolayer. This approach to peptide topology is valid only if the peptide does not induce "flip-flop" of the lysoMC across bilayer. As described in detail elsewhere (*32*), this possibility is controlled for in separate experiments that involve measurements of exchange (or lack of) with the addition of vesicles labeled with nonexchangeable NBD-PE, which quenches lysoMC fluorescence. In the topology experiments presented here, the peptide and lipid concentrations used were 5 μM and 0.3 mM, respectively.

Reversibility of Binding/Insertion. This was assessed by measuring the exchangeability of TMX-1 after it had been incubated with POPC or POPG lipid vesicles for several hours. Two measurements were performed in parallel. In one, peptide-free vesicles labeled with the quencher 7-doxyl-PC (10 mol %) were added to a solution of unlabeled vesicles with bound TMX-1, while in the other, unlabeled peptide-free vesicles were added to a solution of 7-doxyl-PC-labeled vesicles with bound TMX-1. In the first case, free peptide exchange with the added acceptor vesicles should cause Trp quenching by 7-doxyl-PC and consequently a decrease in fluorescence intensity. In the second, free exchange with the unlabeled acceptor vesicles should cause an increase in fluorescence. This parallel procedure provided a pair of solutions of identical composition whose only difference was the order of addition of the labeled and unlabeled acceptor vesicles. Full and reversible peptide exchange was assumed if the fluorescence intensity was intermediate to the original intensities and identical in the two final solutions. Nonexchangeability was assumed if the initial fluorescence levels of the two samples was unaffected by the addition of peptide-free vesicles. In practice, labeled and unlabeled vesicles were added to identical solutions of TMX-1 and fluorescence spectra recorded after incubation for several hours. TMX-1 fluorescence was found to be quenched by about 30% by the presence of the doxyl-labeled lipids.

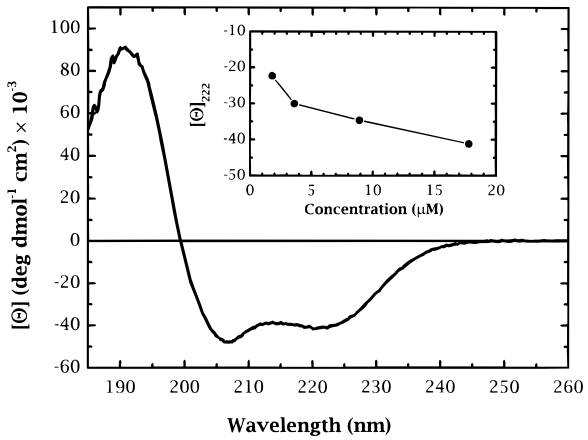

FIGURE 3: Circular dichroism of TMX-1 in buffer. CD spectra were measured for TMX-1 diluted from a 1 mM methanol solution into a 1 mm cuvette containing 50 mM KPO_4 buffer, pH = 7. Peptide concentrations were determined by HPLC after the CD measurements. Inset: Concentration dependence of TMX-1 molar ellipticity at 222 nm.

RESULTS

TMX-1 in Buffer

Circular Dichroism Spectroscopy. TMX-1 did not precipitate when dissolved in buffer; clear solutions were obtained at concentrations up to 300 μM peptide (1 mg/mL). Circular dichroism spectroscopy revealed characteristic α-helix spectra (Figure 3) whose ellipticity depended strongly on concentration (inset, Figure 3), suggesting the formation of aggregates. We concluded, however, that the aggregates were molecular in size because centrifugation at 1000*g* for 10 min, which removes precipitated hydrophobic peptides from solution (*13*), had no effect on the spectra. Furthermore, a strong concentration dependence of the helicity would not be expected for macroscopic aggregates.

From the ellipticity at 222 nm (*42*), we estimated helicities of about 55% at 1 μM and greater than 95% at 17 μM (inset, Figure 3), but we note that the contribution of the Trp residue can obscure precise quantitation of molar ellipticities in helical peptides (*43*). This coupling of helicity to aggregation is reminiscent of that observed for coiled-coils (*44*−*46*). Because the helicity of TMX-1 declined monotonically with concentration, the conformation of the monomer, if it were

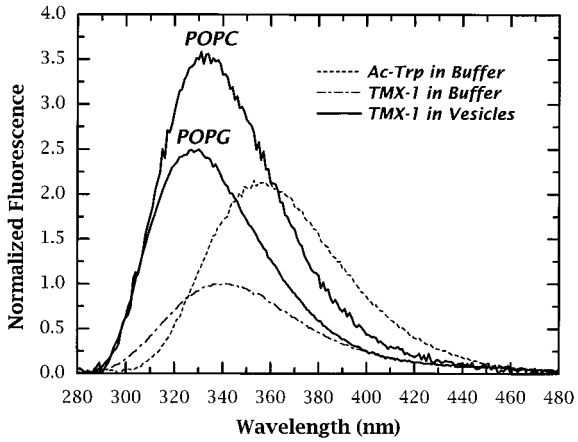

FIGURE 4: Fluorescence of TMX-1 in membranes. Shown are fluorescence emission spectra for 5 μM TMX-1 in buffer and when mixed with 1 mM POPC or POPG vesicles. For comparison we also show the emission spectrum of Ac-Trp in buffer. All intensities have been divided by the molar concentration of Trp in each sample. Samples containing vesicles were preincubated for 3 h prior to making measurements. In all cases, an appropriately scaled (*35*) fluorescence background spectrum obtained from peptide-free vesicles has been subtracted from the raw spectra.

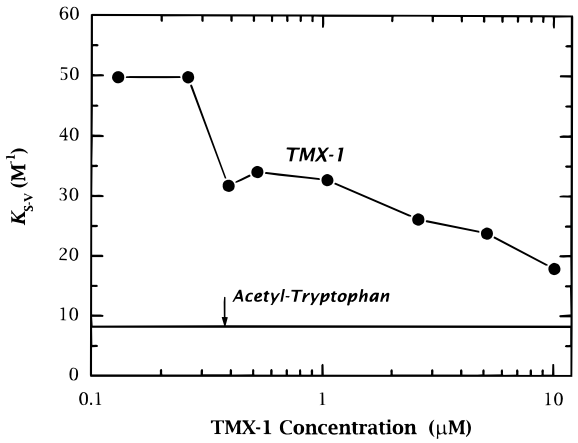

FIGURE 5: Quenching of Trp fluorescence by iodide, I^-. Fluorescence at 340 nm was monitored for solutions of TMX-1 in buffer during titration of a 4 M solution of KI into the cuvette. KI concentrations never exceeded 50 mM. Stern−Volmer constants K_{S-V} were calculated from the slopes of plots of the ratio of unquenched to quenched fluorescence against the molar concentration of KI. Measurements made at TMX-1 concentrations above 5 μM TMX-1 gave rise to slightly curved Stern−Volmer plots, indicating structural heterogeneity. In these cases, K_{S-V} was calculated from the initial slope over the range of 0−20 mM KI. In heterogeneous systems, the initial-slope values are always for the most quenchable population of tryptophan.

observable, would likely be much less helical and could even be random coil. However, the AGADIR algorithm (*25*−*28*) predicts 65% helicity for the monomer (see previous section Design Features of TMX-1), suggesting that the helicity of ~55% observed at 1 μM may be close to that of the monomer.

Fluorescence Spectroscopy. Because the experimentally accessible concentration range for fluorescence measurements is lower than for CD, the aggregation of TMX-1 was studied further by using the intrinsic Trp fluorescence in order to determine if there was any experimentally accessible concentration range between 0.1 and 10 μM at which TMX-1 was monomeric. To do this, we compared the fluorescence properties of the *N*-acetylated Trp of TMX-1 to that of free *N*-acetyltryptophan (*13*), as shown in Figure 4. Over the concentration range of 0.1−10 μM peptide, the λ_{max} for the TMX-1 Trp fluorescence increased only slightly, from 341.8 to 343.4 nm, indicating a very weak dependence of fluorescence on concentration and hence no clear monomer−multimer transition. This wavelength range was significantly blue-shifted compared to the value of 351 nm found for Ac-Trp in buffer, consistent with aggregation. In addition, the quantum yield of TMX-1 relative to that of acetyl-Trp increased from 0.25 to 0.35 over the same concentration range. For comparison, tryptophans that are completely buried within globular proteins typically have emission maxima between 320 and 330 nm, those that are partially buried have maxima between 330 and 345 nm, and fully exposed tryptophans have maxima between 345 and 355 nm (*47*). Our results therefore suggest that the Trp in TMX-1 was partially shielded from the aqueous phase.

We further characterized the aggregates through measurements of the quenching of TMX-1 fluorescence by the anionic, water-soluble quencher iodide, I^-. The quenching results, expressed in terms of Stern−Volmer constants (K_{S-V}) are shown in Figure 5. Trp accessibility to water in this type of experiment is generally thought to be the primary determinant of K_{S-V}. Typically, fully exposed Trp residues have K_{S-V} of 8−9 M^{-1} (*13*), as shown for Ac-Trp in Figure 5, whereas K_{S-V} for buried or inaccessible tryptophans is lower and can be close to 0 M^{-1} (*48*). As expected for aggregation, K_{S-V} depended strongly upon TMX-1 concentration. Surprisingly, however, K_{S-V} was larger (18−50 M^{-1}) than for fully exposed tryptophan. We speculate that this was a result of the proximity of the N-terminal tryptophans to the cationic C-terminal lysines, which increased the local I^- concentration, and perhaps energy transfer between tryptophans. If this speculation is correct, then the results suggest a head-to-tail (antiparallel) helical-bundle arrangement of the aggregates. In any case, the high quenchability of TMX-1 fluorescence with I^- demonstrates unequivocally exposure of a significant fraction of the N-terminal Trp residues to the aqueous phase at all concentrations studied. More importantly, the decrease in K_{S-V} with increasing TMX-1 concentration is consistent with aggregation-induced changes. The abrupt shift in K_{S-V} in Figure 5 suggests a possible change in the structure of the aggregates at about 0.4 μM.

A more complete description of the aggregates could possibly have been obtained by the use of other quenchers such as Cs^+ or acrylamide that should interact differently with the lysine. Analytical ultracentrifugation would have been useful as well. Such experiments were not attempted because our only interest in this exploratory work was to detect aggregation should it exist. A major goal for future TMX peptides is to eliminate aggregation within a concentration range that permits accurate measurements of monomer partitioning.

TMX-1 Interactions with Lipid Membranes

Binding to Vesicles. An important question was whether the free energy of association of TMX-1 in aggregates was sufficiently strong to preclude significant membrane association. We therefore examined the interactions of these aggregates with membrane vesicles made from zwitterionic POPC and from anionic POPG. Attempts to quantitate

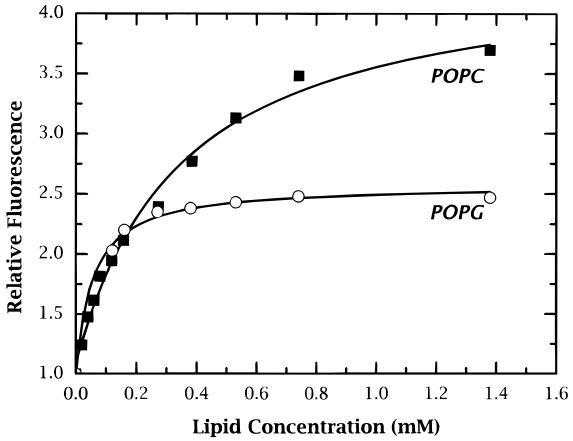

FIGURE 6: TMX-1 binding to vesicles determined from Trp fluorescence. The fluorescence intensity at the emission maxima were measured for 5 μM solutions of TMX-1 as POPC or POPG vesicles were titrated into the cuvette. The maximum is at 328 nm for POPC and 326 nm for POPG. Although the complete binding of TMX-1 to an excess of POPC required more than an hour to complete, we found that the changes accompanying these small titrations were essentially complete after approximately 15 min. We therefore waited at least 20 min after each titration before making the fluorescence measurements.

partitioning of TMX-1 into vesicles by equilibrium dialysis (*35*) failed because TMX-1 equilibrated too slowly across the 14 000 molecular weight cutoff of the dialysis membranes. We turned instead to the use of TMX-1 Trp fluorescence. As shown in Figure 4, relative to fluorescence in buffer, the λ_{max} of TMX-1 (10 μM) shifted dramatically toward the blue in the presence of 1 mM POPC or 1 mM POPG LUV. Specifically, λ_{max} decreased by more than 12 nm and the fluorescence intensity increased by at least 3-fold, consistent with the movement of TMX-1 into an environment in the vesicle bilayers that was more nonpolar than that of the aggregates.

We could thus use fluorescence titration (*35*) to measure TMX-1 partitioning quantitatively by measuring fluorescence intensity at the λ_{max} of the lipid-bound state as lipid vesicles were titrated into an aqueous solution of TMX-1. The partitioning isotherms of Figure 6 show that TMX-1 partitioned strongly into both POPC and POPG vesicles and was mostly bound at lipid concentrations of about 1 mM or less. Assuming a two-state equilibrium between water-soluble aggregates and membrane-bound peptide and ignoring possible differences between the quantum yields of TMX-1 monomers and aggregates in the aqueous phase, the apparent mole fraction partition coefficients were determined (*35*) by fitting the binding curves to the equation $I = f_{bound}I_{max} + (1 - f_{bound})I_0$, for which I is the relative fluorescence intensity, I_0 is the intensity in the absence of lipid, and $f_{bound} = K_xL/(W + K_xL)$, where K_x is the mole-fraction partition coefficient, L is the lipid concentration, and W is the molar concentration of water (55.3 M at 25 °C). For POPC, $K_x = (1.6 \pm 0.2) \times 10^5$, and for POPG, $K_x = (1.0 \pm 0.2) \times 10^6$. These correspond to $\Delta G = -7.1 \pm 0.1$ kcal mol^{-1} and -8.2 ± 0.1 kcal mol^{-1}, respectively ($\Delta G = -RT \ln K_x$). We caution that these values have uncertain meaning because of the aggregation of TMX-1 in buffer. The free energy of partitioning into POPG vesicles is especially problematic because the interaction did not appear to be reversible on the time scale of the experiments (see below). A proper accounting of the free energy requires proof of reversibility, knowledge of the aggregate composition and concentration, and the concentration and structure of monomeric peptide. Nevertheless, the apparent values of ΔG are likely to represent lower limits for the energetics of TMX-1 partitioning into vesicles.

Structure of TMX-1 in Membranes. We found that, when completely bound to POPC and POPG vesicles, the molar ellipticity of TMX-1 (data not shown) was essentially identical to that of TMX-1 in buffer at a concentration of 17 μM peptide (Figure 3). Specifically, the molar ellipticity of TMX-1 at 222 nm in buffer or in POPC is $-41\,000 \pm 1000$ deg dmol^{-1} cm^2, while in POPG it is $-39\,000 \pm 1000$ deg dmol^{-1} cm^2. The ellipticities in vesicles were independent of peptide concentration.

These ellipticities indicate that TMX-1 is nearly fully helical when bound to vesicles. Because this helicity could arise from two populations of TMX-1, i.e., transmembrane and surface-bound, a critical question was the thermodynamic feasibility of the transmembrane form. To address this question, we performed oriented circular dichroism (OCD) measurements on TMX-1 in oriented multibilayers of POPC or POPG that form spontaneously on quartz slides after deposition from a methanol solution of lipid and peptide (*49*). Following solvent removal and hydration via the vapor phase, slides were oriented with the plane of the membranes normal to the beam axis (see Materials and Methods). Because the ellipticity of peptide absorption bands depends on their orientation with respect to this optical axis (*41*), the OCD spectra of transmembrane helical peptides are very different from the spectra of α-helices lying parallel to the membrane surface, as illustrated by the computed theoretical spectra (*41*) shown in Figure 7A (inset). These computed spectra show that transmembrane helices have a single minimum at 225 nm and a maximum at 195 nm, while surface helices have minima at both 208 and 225 nm and a maximum at 190 nm. We confirmed the spectral shape and band positions for helices parallel to the surface by examining a number of highly charged model amphipathic helices (*32*, *50*, *51*), which were expected to be parallel to the bilayer surface. All of the amphipathic peptides were found to have two minima of approximately equal ellipticity, one at 208 nm and one at 225 nm, consistent with a surface orientation. The orientation of one of these peptides, Ac-18A-NH_2, has been confirmed directly by a novel X-ray diffraction method (*52*).

The observed OCD spectra for TMX-1 in both POPC and in POPG had the characteristic shape and extrema positions expected for transmembrane helices (Figure 7, panels A and B, respectively). The shoulder at 208 nm in panel B suggests the possibility of a small fraction of surface helix or nonhelical secondary structure in POPG, but from numerical simulations we estimated this fraction to be no more than 15%. Alternately, a helical tilt of ~20° could account for this observed shoulder. These possibilities could not be distinguished experimentally. The TM orientation of TMX-1 is probably a thermodynamically stable state in oriented multilayers because the OCD spectra were independent of the peptide/lipid ratio from 1:10 to 1:50, hydration varying from 0 to 100% RH, and sample incubation times varying from 10 min to 48 h. Although there are obvious differences between oriented multilayer and vesicle bilayers in terms of formation mechanism and local microscopic environment,

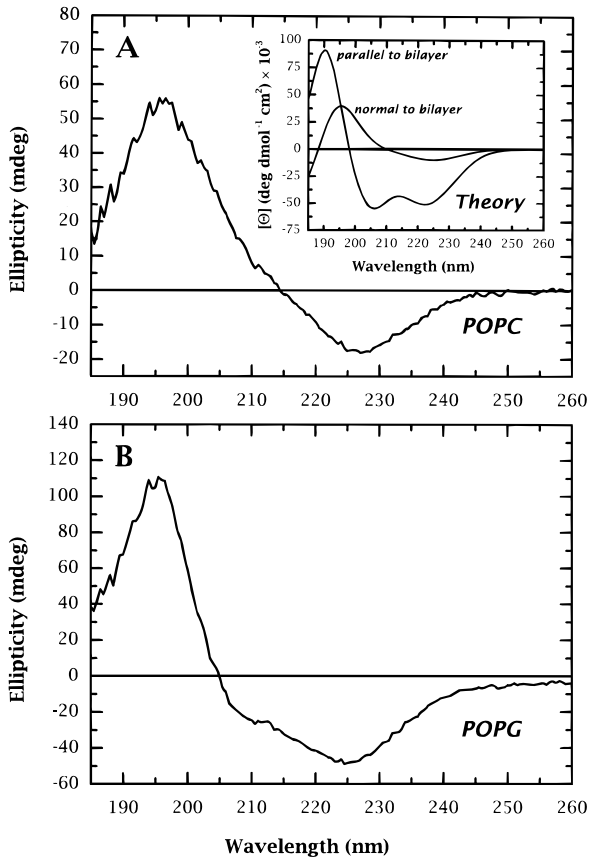

FIGURE 7: Oriented circular dichroism (OCD) spectra of TMX-1 in oriented POPC (panel A) and POPG (panel B) multilayers. Samples were prepared as described under Materials and Methods. The inset of panel A shows the OCD spectra expected for helices oriented parallel and normal to the bilayer plane computed from the equations of Huang and colleagues (*39*−*41*). The correctness of the parallel spectrum has been verified through X-ray diffraction measurements (*52*). The spectra for TMX-1 in both POPC and POPG multilayers are very similar to those expected for the normal orientation.

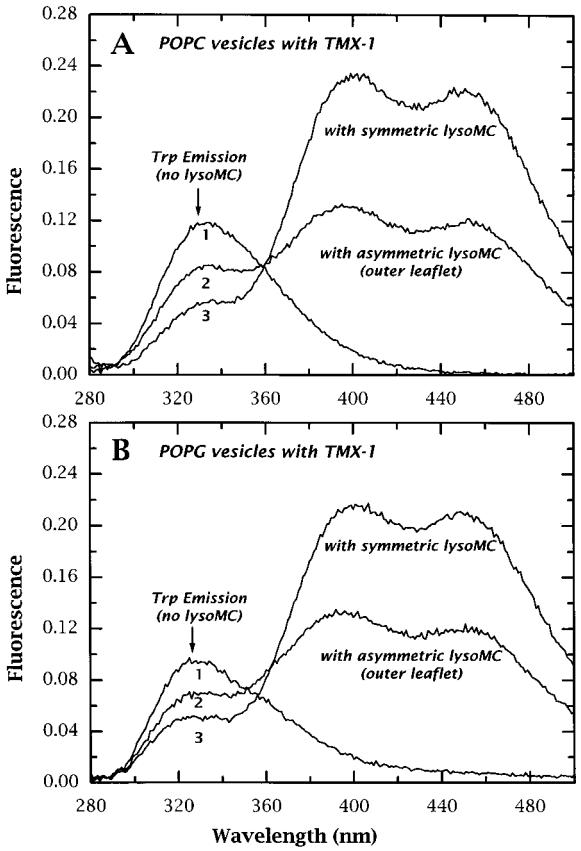

FIGURE 8: Determination of peptide topology in POPC vesicles (panel A) and POPG vesicles (panel B) using the RET quencher lysoMC. The assay is described briefly under Materials and Methods and in detail elsewhere (*32*). The curves in each panel labeled 1, 2, and 3 show, respectively, the Trp fluorescence of TMX-1 in the absence of lysoMC, in the presence of asymmetrically distributed lysoMC, and in the presence of symmetrically distributed lysoMC. The difference in Trp fluorescence between curves 2 and 3 reveals the topology of the peptide's tryptophan (*32*). In this case, about half of the TMX-1 Trp residues translocate across to the opposite side of the membrane. See text for further discussion.

the dominance of the TM orientation in oriented multilayers strongly supports the thermodynamic feasibility of a significant transmembrane population of TMX-1 bound to vesicles. Two critical questions were next addressed: (1) Did a significant fraction of TMX-1 insert spontaneously into vesicles with a TM orientation and (2) was the insertion reversible?

Topology of TMX-1 in Vesicles. The first question was addressed with a novel fluorescence quenching assay for topology (*32*) that utilizes the lysolipid-linked quencher lysoMC (see Materials and Methods). The results of the assay for TMX-1 in POPC and POPG LUV, consisting of three fluorescence emission curves, are shown in Figure 8, panels A and B, respectively. Each curve shows the fluorescence of Trp (left peaks) and the RET-induced fluorescence of the coumarin moiety of lysoMC (right peaks). The topology of Trp could be inferred from the intensities of Trp emission peaks, as follows.

The curves labeled 1 are the Trp fluorescence of TMX-1 in vesicles lacking lysoMC. Curves labeled 2 show the Trp fluorescence of TMX-1 in vesicles containing 1 mol % lysoMC in the outer monolayer of the vesicles (asymmetric lysoMC), and curves labeled 3 show the fluorescence in vesicles containing 1 mol % lysoMC symmetrically distributed in both monolayers. For both POPC and POPG vesicles, Figure 8 shows that the level of Trp fluorescence is different in the presence of symmetric and asymmetric lysoMC. The level of quenching for symmetric lysoMC is a measure of the maximum possible quenching of the tryptophans because they will be quenched regardless of which bilayer leaflet they reside in. If the N-terminus Trp of TMX-1 had not crossed the membrane, then asymmetric lysoMC in the outer bilayer leaflet would have quenched Trp to the same extent as in the symmetric case. We observed, however, that the quenching level was lower (i.e., the Trp fluorescence was higher) in the asymmetric case. This means that some of the N-terminal tryptophans moved across the vesicle membranes to the inside monolayer where they were less accessible to the lysoMC on the outer monolayer. Because the C-terminus of TMX-1 carries four positive charges, it should not have been able to cross the membrane. The translocation of the Trp residue thus suggested that TMX-1 inserted across the membrane as a transbilayer helix. We estimate from the difference in quenching between the symmetric and asymmetric vesicles that roughly 50% of the Trp residues crossed the membrane (*32*), consistent with the thermodynamic feasibility established by the OCD measurements.

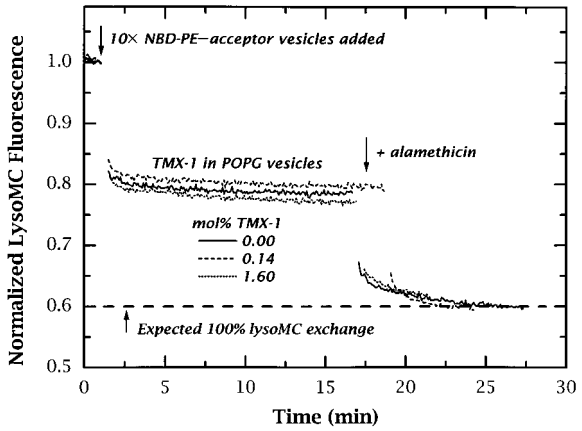

FIGURE 9: Demonstration that TMX-1 does not cause transmembrane flip-flop of lysoMC in POPG. Similar results were obtained for POPC (data not shown). Acceptor vesicles, containing the quencher NBD-PE, added to vesicles containing bound TMX-1 caused the lysoMC fluorescence to fall to about half of the value expected for complete exchange of all lysoMC with the acceptor vesicles. The addition of alamethicin, which has been shown to cause lysoMC flip-flop (*32*) causes the further reduction of lysoMC fluorescence to the 100% exchange level. These results demonstrate that TMX-1 does not cause the lysoMC located on the inner monolayer leaflet to flip to the outer leaflet. See text for further discussion.

These conclusions would not be valid if TMX-1 caused the lysoMC to flip-flop across the membranes. The control experiments (*32*) of Figure 9 demonstrate that lysoMC flip-flop did not occur in POPG vesicles in the presence of TMX-1. Similar data were obtained for POPC (not shown). In these control experiments, TMX-1 was partitioned into vesicles symmetrically labeled with lysoMC, which was excited directly at its absorbance maximum of 340 nm. The resulting normalized fluorescence is shown at the far left of Figure 9 for POPG. Peptide-free NBD-PE-labeled acceptor vesicles, added at about 1 min (Figure 9), caused the lysoMC fluorescence level to drop to a new steady-state level because some of the lysoMC moved to the acceptor vesicles where it was quenched by the nonexchangeable NBD-PE. We have demonstrated (*32*) that the addition of alamethicin to vesicles symmetrically labeled with lysoMC causes flip-flop and consequently complete loss of lysoMC to acceptor vesicles. As shown in Figure 9, the subsequent addition of alamethicin caused a further decrease in lysoMC fluorescence to the level expected for 100% lysoMC exchange. A comparison of the pre-alamethicin fluorescence level with the post-alamethicin level in Figure 9 demonstrates that only 50% of the lysoMC (i.e., that in the outer bilayer leaflet) was exchangeable in the absence of alamethicin. We therefore concluded that TMX-1 did not cause lysoMC to equilibrate across bilayers. The data of Figure 9 show that this conclusion was unaffected by the concentration of TMX-1 in the donor vesicles.

Reversibility of TMX-1 Insertion. This question was examined by measuring the exchangeability of TMX-1 between vesicles. Two types of vesicles were prepared: Pure vesicles (POPG or POPC) and vesicles containing 10 mol % of the nonexchangeable Trp fluorescence quencher 7-doxyl-PC. The experiment proceeded by partitioning TMX-1 into one type of vesicle (3 h equilibration period) and measuring the Trp fluorescence before and after the addition of the other type. An experiment that demonstrates reversibility for TMX-1 partitioning into POPC vesicles is

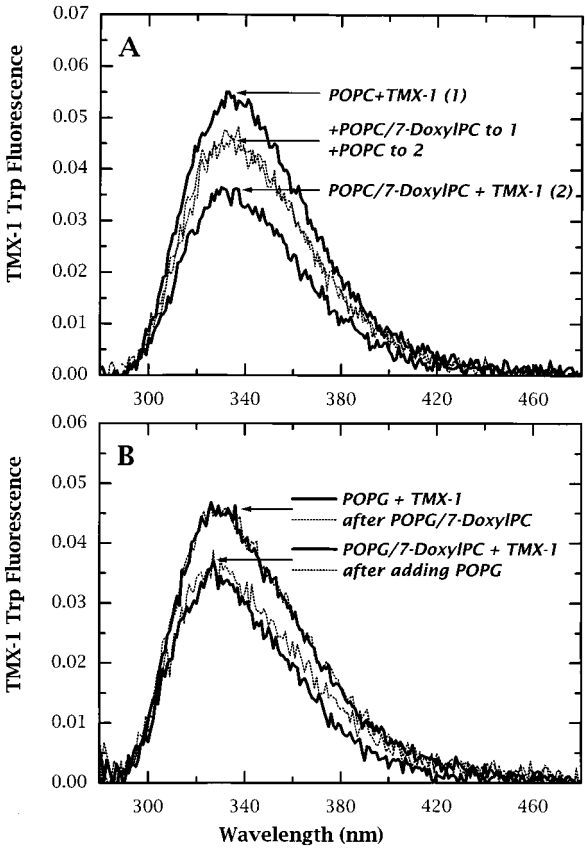

FIGURE 10: Test of the reversibility of TMX-1 binding to POPC (panel A) and POPG (panel B) vesicles. In these experiments, we first measured the tryptophan emission spectra in pure lipid vesicles and in vesicles containing 10 mol % of the nonexchangeable lipid quencher 7-doxyl PC. These are the upper and lower curves in the panels. Note that 7-doxyl PC quenches TMX-1 fluorescence by about 30%. We then added to the pure lipid samples the same amount of quencher-containing vesicles and to the quencher-containing samples the same amount of pure lipid vesicles. This gave two identical solutions whose only difference was the order of addition of the vesicle types. After several more hours of incubation, the emission spectra are remeasured. Comparison of the second spectra to the initial ones reveals whether the peptide exchanges between the vesicles on these time scales. As described in greater detail in the text, TMX-1 readily exchanges between POPC vesicles but not POPG vesicles.

shown in Figure 10A. The top solid curve shows the TMX-1 Trp fluorescence in pure POPC vesicles and the lower solid curve shows the fluorescence in POPC/7-doxyl-PC vesicles. The fluorescence in the latter case was lower because of the 7-doxyl-PC quenching. The addition of pure POPC vesicles caused the fluorescence in this case to increase (dotted curves) with a time constant of less than 3 h as a result of the loss of TMX-1 from the POPC/7-doxyl-PC vesicles to the pure POPC vesicles. The same level of fluorescence was observed when the order of the experiment was reversed. That is, fluorescence decreased when POPC/7-doxyl-PC vesicles were added to POPC-only vesicles containing TMX-1. This demonstrates the reversibility of TMX-1 partitioning because the intermediate level of fluorescence was unaffected by the order in which the experiments were performed. By this criterion, Figure 10B shows that TMX-1 partitioning was not reversible for POPG vesicles because the initial fluorescence spectra observed were unaffected by the addition of the opposite type of vesicle. Other peptides bound to membranes by strong electrostatic interactions have also been

found to be nonexchangeable on these time scales (*53*).

Elimination of Fusion Events as the Cause of Exchangeability. We used two fluorescence methods, NBD/rhodamine-labeled lipids (*54*) and lysoMC/NBD-PE quenching (*32*), to eliminate the possibility that vesicle fusion was responsible for the apparent exchange of TMX-1 between POPC vesicles. For example, we mixed 2 mol % TMX-1 with vesicles containing 1 mol % NBD-PE and then added a 10-fold excess of vesicles containing 1 mol % rhodamine-PE quencher. Fusion of these vesicles should have caused NBD fluorescence to be strongly quenched (*54*), but after several hours of incubation the NBD-PE fluorescence was identical to that measured in the absence of TMX-1 or before the addition of rhodamine-containing vesicles.

As a secondary control experiment, we subjected these same vesicles to multiple freeze−thaw cycles, a procedure known to induce vesicle fusion (*55*). We found, as expected, that the NBD-PE fluorescence decreased substantially and the Rho-PE fluorescence increased accordingly. Similar experiments with lysoMC/POPC and NBD-PE/POPC vesicles (*32*) confirmed that TMX-1 did not cause fusion of POPC or POPG at the concentrations used in these experiments. The apparent nonexchangeability of TMX-1 in POPG (panel B of Figure 9) ruled out fusion in that system. We thus conclude that no vesicle fusion occurred and that fusion cannot explain the apparent exchangeability of TMX-1.

DISCUSSION

In order for a family of host−guest peptides to be useful for thermodynamic measurements, the basic requirements are (1) measurable solubility in water as monomers, (2) ability to form transmembrane α-helices, and (3) strong and reversible binding to membranes. TMX-1 was intended as the first step toward designing peptides that meet these requirements. The results presented above are encouraging in that TMX-1 had many of the properties envisioned in its design. The first requirement was the most problematic, as expected.

TMX-1 in the Absence of Membranes. The most encouraging result was that TMX-1 did not precipitate or otherwise form macroscopic aggregates in the absence of membranes. Like many other membrane-active biological peptides and proteins, TMX-1 apparently circumvented precipitation through the formation of molecular aggregates that reduce the water accessibility of nonpolar surfaces. The bee venom peptide melittin, for example, forms helical tetramers (*56*), and the bacterial toxin colicin A buries its membrane-inserting hydrophobic helices within a set of more hydrophilic ones (*57*).

Although we chose not to explore in detail the structure of the molecular aggregates in water (studies of the effects of temperature and ionic strength would have been useful, for example), the data obtained suggest aggregates organized around an antiparallel helical-bundle motif. An accidental feature of the design of TMX-1 (Figure 2) was the placement of alanines at (i, $i + 7$) in the sequence (positions 3, 10, and 17), which strongly promotes very tight antiparallel coiled-coils ("Alacoil" motif) with helix-axis separations of less than 8.5 Å (*58*). Interestingly, the helix crossing angle of Alacoils, like soluble coiled-coils (*59*), is ∼+20°, similar to the antiparallel helical bundles observed in membrane proteins (*60*), which are generally less tightly packed (helix axis separations of ∼9.6 Å). The CD spectra of TMX-1 (Figure 3) and the fluorescence quenching by I^- (Figure 5) are consistent with some kind of antiparallel coiled-coil arrangement that brings the Trp residues into proximity with the Lys residues. We speculate that the fundamental "solubility unit" may be a dimer, but because the helicity of TMX-1 declines dramatically at low concentrations (∼1 μM), the coiled-coil in such a case would either have to be rather loose and somewhat disordered over its entire length or zipped tightly only over part of its length. Favorable dimer solubility may arise from the combination of burial of nonpolar side chains, which can be quite significant in dimers (*59*), and exposure of the lysines. The formation of higher multimers with higher helicity at elevated peptide concentrations may be favored by burial of additional nonpolar surface but opposed by the proximity of the C-terminal Lys residues. Overall, the image of TMX-1 that emerges is one in which there is a distribution of helix-bundle sizes that shifts between smaller and less helical states to larger, more helical structures as peptide concentration is increased. The results suggest that there may be a concentration in the nanomolar range at which TMX-1 is monomeric. Although this concentration is too low for most biophysical studies, it suggests that TMX-1 may not be far from fulfilling the first design requirement, namely, solubility as a monomer in water. A titratable His residue placed near the center of the helix, for example, may be useful for preventing aggregation.

TMX-1 in Membranes. The data of Figure 6 show that TMX-1 partitioned strongly into both POPC and POPG vesicles, despite its formation of molecular aggregates in the aqueous phase. This means that the free energy of association of TMX-1 with membranes was much more favorable than its association with aqueous aggregates. The fluorescence quenching experiments designed to examine the exchange of TMX-1 between vesicles (Figure 10) showed, however, that TMX-1 associates reversibly only with POPC vesicles, at least on the time scale of the experiments. The CD spectra of TMX-1 in vesicles was quantitatively equivalent to the spectrum of TMX-1 at 17 μM in water (Figure 3), indicating a helicity of greater than 90%. Therefore, TMX-1 in all forms, i.e., TM and surface-bound, was predominantly α-helical.

The OCD measurements (Figure 7) showed that the TM orientation was more strongly preferred in oriented multilayers formed from both POPC and POPG. We estimate from the ratio of the ellipticities at 208 and 225 nm (*41*) that the transmembrane population of TMX-1 was greater than 90% in POPC and at least 85% in POPG. We concluded that the transmembrane insertion of TMX-1 into vesicles was thermodynamically feasible. Consistent with this conclusion, the lysoMC topology measurements demonstrated for spontaneously partitioned TMX-1 that about 50% of the Trp residues crossed the membrane, implying a significant TM population of TMX-1 in both POPC and POPG vesicles after a 24-h equilibration (Figure 8).

There are several possible explanations for this incomplete TM insertion. One possibility is a true equilibrium between surface-bound and inserted peptide. For POPC at least, this is supported by the fact that binding and insertion were fully reversible. Alternately, the noninserted peptide could be in a kinetically trapped state such as surface-bound aggregates resulting from the intentional placement of the Leu and Val

residues in the sequence to create a mildly amphipathic helix. Another possibility is that transmembrane insertion is a stochastic process that occurs only during the initial stages of kinetically trapped binding. This has often been proposed as an explanation of the kinetic deactivation of pore-forming peptides in vesicle leakage assays (*61*, *62*). Although the strong partitioning of TMX-1 into vesicles (Figure 6) argues against it, the helices may have inserted cooperatively as antiparallel helical pairs or bundles. TM insertion of 100% of the peptide in that case would place 50% of the Trp residues on the inner monolayer. Unfortunately, the design of TMX-1 precluded facile determination of the topology of its C-terminus. Future designs must allow for such measurements.

TMX-1 partitioned into zwitterionic POPC and anionic POPG vesicles with apparent mole-fraction free energies values of -7.1 and -8.2 kcal mol^{-1}, respectively (Figure 6). However, because partitioning into POPG vesicles was not reversible on the time scale of our experiments (Figure 10), equilibrium thermodynamics can be considered only for the case of POPC partitioning. Even then, the ΔG value represents composite numbers that reflect the equilibrium between the aggregated forms in water and the membrane-bound forms (Figure 1B). These complications make it impractical to propose a specific molecular interpretation of the apparent ΔG values, but the fact that they fall into the readily measurable range (*35*) is encouraging. Nevertheless, the numbers we obtain for TMX-1 are similar to those of other, more uncertain experiments. For instance, Moll and Thompson (*18*) calculated ~ -5 kcal/mol for the membrane binding of Ala_{20} linked to the hydrophilic carrier protein BPTI, Soekarjo et al. (*19*) calculated -12 kcal/mol for the insertion of one of the transmembrane helices of the M13 coat protein, and Hunt et al. (*64*) calculated -6 kcal/mol for the binding and insertion of a sequence corresponding to the C-helix of bacteriorhodopsin. In all these cases, as discussed in detail elsewhere (*1*, *22*), the final values for ΔG have uncertain significance because of aqueous phase aggregation, unknown secondary structure, inability to distinguish between surface binding and insertion, and failure to establish that the degree of binding or insertion was an equilibrium effect and not a kinetic one. These are some of the same fundamental difficulties that also make the interpretation of the TMX-1 results uncertain.

What values of ΔG might be expected for TMX-1 partitioning and insertion into phosphatidylcholine membranes? Some estimates, and we must emphasize that they are only estimates, can be obtained from our experimentally determined whole-residue hydrophobicity scales (*1*, *22*) for partitioning into POPC interfaces (*16*) and into *n*-octanol (*13*) and from recent determinations of the energetics of secondary structure formation in POPC interfaces (*38*, *65*). The free energy[3] ΔG_{wiu} of partitioning the unfolded 21 amino acid hydrophobic span of TMX-1 into the POPC interface is estimated from the interfacial hydrophobicity scale as $+1.1$ kcal mol^{-1} and the free energy reduction ΔG_{if} associated with folding as -8.4 kcal mol^{-1}, based upon energy reduction per residue ($\Delta G_{residue}$) of -0.4 kcal mol^{-1} associated with melittin folding (*65*). Assuming the existence of monomeric TMX-1 in the aqueous phase, which may not be unreasonable for f_{bound} approaching 1 (Figure 6), the net free energy of partitioning the folded peptide would thus be $\Delta G = \Delta G_{wiu} + \Delta G_{if} = -7.3$ kcal mol^{-1}. This value is remarkably, and probably fortuitously, close to the observed value for POPC partitioning. (If the N-terminal Trp and Asn residues of TMX-1 are included, then the free energy values are -0.35, -9.2, and -9.6 kcal mol^{-1}.) If there is a 1:1 distribution of folded TMX-1 between interfacial and TM locations, as our data suggest may be true, the free energy of transfer ΔG_{ihf} for inserting the peptide from the interface would be 0. That is, the free energy of transferring unfolded TMX-1 from water to an α-helical TM configuration would also be -7.3 kcal mol^{-1}.

We have suggested (*1*) that the transfer free energy ΔG_{Hbond} of an H-bonded peptide bond into a pure hydrocarbon phase may be approximately equal to the free energy of transfer ΔG_{glycyl} of a non-H-bonded peptide bond into octanol. This was suggested because (1) the H-bonding of the glycyl unit to the hydroxyl might be energetically equivalent to the H-bonding in α-helices and (2) $\Delta G_{glycyl} = +1.15$ kcal mol^{-1} falls squarely between the upper (*66*) and lower (*15*) estimates of ΔG_{Hbond} (2.0 and 0.6 kcal mol^{-1}, respectively). This reasoning implied, therefore, that our whole-residue *n*-octanol hydrophobicity scale may provide a reasonable first estimate for the transfer free energy ΔG_{whf} of a TM helix from water to the bilayer hydrocarbon core. Making that assumption for the hydrophobic span of TMX-1, we found that $\Delta G_{whf} = +1.13$ kcal mol^{-1}. This unfavorable value suggests that the octanol-scale ΔG_{glycyl} overestimates ΔG_{Hbond}. As an illustration of the importance of having a reliable experimental measurement of ΔG_{Hbond}, we note that the use of the lower estimate (*15*) would reduce the cost of ΔG_{Hbond} implicit in the *n*-octanol scale by about 0.5 kcal mol^{-1} per residue and hence change ΔG_{whf} to a very favorable value of about -9 kcal mol^{-1}.

This study of TMX-1 and the above calculations reveal the complexity of the problem of determining the energetics of folding proteins into membranes. Our experience with TMX-1 convinces us, however, that the experimental determination of these energetics is within reach. Future designs of TMX peptides must address three issues. First, the monomer solubility must be brought into an experimentally useful range without sacrificing the ability of TMX to partition and insert. One possibility would be to increase slightly the hydrophobicity of the hydrophobic span and at the same time introduce a His residue in order to enhance aqueous solubility and retard aggregation. This would allow the second issue to be addressed, namely, the need to bring the wide range of equilibrium constants inherent in Figure 1 into a measurable regime. Changes in pH could be used to control the equilibrium among the states shown in Figure 1. Third, the composition of the C-terminal sequence must be modified so that its topology can be determined. This could be an enzyme-sensitive site, for example, or a specifically reactive residue.

[3] Subscript conventions (*1*): w = water, i = interface, h = hydrocarbon core, u = unfolded, and f = folded; e.g., wiu is read as water-to-interface in the unfolded form. See also http://blanco.biomol.uci.edu/peptide_bilayer_energetics.html.

ACKNOWLEDGMENT

We thank Drs. Kalina Hristova and Alexey Ladokhin for many enlightening discussions, Dr. Michael E. Selsted for

the use of his peptide synthesizer, and Mr. Dat Tran for his expert assistance in the synthesis. We also acknowledge the assistance of Kaisheng Chen in the early stages of peptide purification, Renee Dillinger for helping with the CD spectroscopy, and Dr. John Greaves for help with the mass spectrometry.

REFERENCES

1. White, S. H., and Wimley, W. C. (1999) *Annu. Rev. Biophys. Biomol. Struct. 28*, 319−365.
2. Shinoda, K., Yamaguchi, T., and Horigome, T. (1961) *Bull. Chem. Soc. Jpn. 34*, 237−241.
3. Wallin, E., and von Heijne, G. (1998) *Protein Sci. 7*, 1029−1038.
4. Boyd, D., Schierle, C., and Beckwith, J. (1998) *Protein Sci. 7*, 201−205.
5. von Heijne, G. (1981) *Eur. J. Biochem. 120*, 275−278.
6. Engelman, D. M., Steitz, T. A., and Goldman, A. (1986) *Annu. Rev. Biophys. Biophys. Chem. 15*, 321−353.
7. White, S. H., and Jacobs, R. E. (1990) *J. Membr. Biol. 115*, 145−158.
8. White, S. H. (1994) in *Membrane Protein Structure: Experimental Approaches* (White, S. H., Ed.) pp 97−124, Oxford University Press, New York.
9. Reithmeier, R. A. F. (1995) *Curr. Opin. Struct. Biol. 5*, 491−500.
10. Lemmon, M. A., and Engelman, D. M. (1994) *Q. Rev. Biophys. 27*, 157−218.
11. Yang, A.-S., Sharp, K. A., and Honig, B. (1992) *J. Mol. Biol. 227*, 889−900.
12. Liu, Y., and Bolen, D. W. (1995) *Biochemistry 34*, 12884−12891.
13. Wimley, W. C., Creamer, T. P., and White, S. H. (1996) *Biochemistry 35*, 5109−5124.
14. Luo, P. Z., and Baldwin, R. L. (1999) *Proc. Natl. Acad. Sci. U.S.A. 96*, 4930−4935.
15. Roseman, M. A. (1988) *J. Mol. Biol. 201*, 621−625.
16. Wimley, W. C., and White, S. H. (1996) *Nat. Struct. Biol. 3*, 842−848.
17. Ben-Tal, N., Ben-Shaul, A., Nicholls, A., and Honig, B. (1996) *Biophys. J. 70*, 1803−1812.
18. Moll, T. S., and Thompson, T. E. (1994) *Biochemistry 33*, 15469−15482.
19. Soekarjo, M., Eisenhawer, M., Kuhn, A., and Vogel, H. (1996) *Biochemistry 35*, 1232−1241.
20. Chung, L. A., and Thompson, T. E. (1996) *Biochemistry 35*, 11343−11354.
21. Morein, S., Strandberg, E., Killian, J. A., Persson, S., Arvidson, G., Koeppe, R. E., II, and Lindblom, G. (1997) *Biophys. J. 73*, 3078−3088.
22. White, S. H., and Wimley, W. C. (1998) *Biochim. Biophys. Acta 1376*, 339−352.
23. Richardson, J. S., and Richardson, D. C. (1988) *Science 240*, 1648−1652.
24. Aurora, R., and Rose, G. D. (1998) *Protein Sci. 7*, 21−38.
25. Muñoz, V., and Serrano, L. (1995) *J. Mol. Biol. 245*, 275−296.
26. Muñoz, V., and Serrano, L. (1995) *J. Mol. Biol. 245*, 297−308.
27. Muñoz, V., and Serrano, L. (1997) *Biopolymers 41*, 495−509.
28. Lacroix, E., Viguera, A. R., and Serrano, L. (1998) *J. Mol. Biol. 284*, 173−191.
29. Li, S.-C., and Deber, C. M. (1994) *Nat. Struct. Biol. 1*, 368−373.
30. Schiffer, M., Chang, C. H., and Stevens, F. J. (1992) *Protein Eng. 5*, 213-214.
31. Yau, W.-M., Wimley, W. C., Gawrisch, K., and White, S. H. (1998) *Biochemistry 37*, 14713−14718.
32. Wimley, W. C., and White, S. H. (2000) *Biochemistry 39*, 161−170.
33. Hope, M. J., Bally, M. B., Mayer, L. D., Janoff, A. S., and Cullis, P. R. (1986) *Chem. Phys. Lipids 40*, 89−107.
34. Mayer, L. D., Hope, M. J., and Cullis, P. R. (1986) *Biochim. Biophys. Acta 858*, 161−168.
35. White, S. H., Wimley, W. C., Ladokhin, A. S., and Hristova, K. (1998) *Methods Enzymol. 295*, 62−87.
36. Wimley, W. C., and White, S. H. (1993) *Anal. Biochem. 213*, 213-217.
37. Selsted, M. E., Harwig, S. S. L., Ganz, T., Schilling, J. W., and Lehrer, R. I. (1985) *J. Clin. Invest. 76*, 1436−1439.
38. Wimley, W. C., Hristova, K., Ladokhin, A. S., Silvestro, L., Axelsen, P. H., and White, S. H. (1998) *J. Mol. Biol. 277*, 1091−1110.
39. Olah, G. A., and Huang, H. W. (1988) *J. Chem. Phys. 89*, 2531−2538.
40. Olah, G. A., and Huang, H. W. (1988) *J. Chem. Phys. 89*, 6956−6962.
41. Wu, Y., Huang, H. W., and Olah, G. A. (1990) *Biophys. J. 57*, 797−806.
42. Luo, P. Z., and Baldwin, R. L. (1997) *Biochemistry 36*, 8413−8421.
43. Chakrabartty, A., Kortemme, T., Padmanabhan, S., and Baldwin, R. L. (1993) *Biochemistry 32*, 5560−5565.
44. Eisenberg, D., Wilcox, W., Eshita, S. M., Pryciak, P. M., Ho, S. P., and DeGrado, W. F. (1986) *Proteins: Struct., Funct., Genet. 1*, 16−22.
45. Ho, S. P., and DeGrado, W. F. (1987) *J. Am. Chem. Soc. 109*, 6751−6758.
46. Handel, T. M., Williams, S. A., and DeGrado, W. F. (1993) *Science 261*, 879−885.
47. Burstein, E. A., Vedenkina, N. S., and Ivkova, M. N. (1973) *Photochem. Photobiol. 18*, 263−279.
48. Liu, L.-P., and Deber, C. M. (1997) *Biochemistry 36*, 5476−5482.
49. Lu, M., and Tjerneld, F. (1997) *J. Chromatogr. A 766*, 99−108.
50. Venkatachalapathi, Y. V., Phillips, M. C., Epand, R. M., Epand, R. F., Tytler, E. M., Segrest, J. P., and Anantharamaiah, G. M. (1993) *Proteins: Struct., Funct., Genet. 15*, 349−359.
51. Mishra, V. K., and Palgunachari, M. N. (1996) *Biochemistry 35*, 11210−11220.
52. Hristova, K., Wimley, W. C., Mishra, V. K., Anantharamaiah, G. M., Segrest, J. P., and White, S. H. (1999) *J. Mol. Biol. 290*, 99−117.
53. Jones, J. D., and Gierasch, L. M. (1994) *Biophys. J. 67*, 1546−1561.
54. Struck, D. K., Hoekstra, D., and Pagano, R. E. (1981) *Biochemistry 20*, 4093−4099.
55. Lentz, B. R., Carpenter, T. J., and Alford, D. R. (1987) *Biochemistry 26*, 5389−5397.
56. Terwilliger, T. C., and Eisenberg, D. (1982) *J. Biol. Chem. 257*, 6016−6022.
57. Parker, M. W., Postma, J. P. M., Pattus, F., Tucker, A. D., and Tsernoglou, D. (1992) *J. Mol. Biol. 224*, 639−657.
58. Gernert, K. M., Surles, M. C., Labean, T. H., Richardson, J. S., and Richardson, D. C. (1995) *Protein Sci. 4*, 2252−2260.
59. Harbury, P. B., Zhang, T., Kim, P. S., and Alber, T. (1993) *Science 262*, 1401−1407.
60. Bowie, J. U. (1997) *J. Mol. Biol. 272*, 780−789.
61. Matsuzaki, K., Murase, O., and Miyajima, K. (1995) *Biochemistry 34*, 12553−12559.
62. Rex, S., and Schwarz, G. (1998) *Biochemistry 37*, 2336−2345.
63. Hunt, J. F., Rath, P., Rothschild, K. J., and Engelman, D. M. (1997) *Biochemistry 36*, 15177−15192.
64. Ladokhin, A. S., and White, S. H. (1999) *J. Mol. Biol. 285*, 1363−1369.
65. Ben-Shaul, A., Ben-Tal, N., and Honig, B. (1996) *Biophys. J. 71*, 130−137.
66. MacKenzie, K. R., Prestegard, J. H., and Engelman, D. M. (1997) *Science 276*, 131−133.

BI992746J